remote sensing

MDPI

Article

C3 Vegetation Mapping and CO_2 Fertilization Effect in the Arid Lower Heihe River Basin, Northwestern China

Yunbo Bi and Hongjie Xie *

Received: 31 July 2015 ; Accepted: date 27 November 2015 ; Published: 4 December 2015
Academic Editors: Xin Li, Yuei-An Liou, Qinhuo Liu, Parth Sarathi Roy and Prasad S. Thenkabail

Laboratory for Remote Sensing and Geoinformatics, Department of Geological Sciences, University of Texas at San Antonio, San Antonio, TX 78249, USA; biyunbo@gmail.com
* Correspondence: hongjie.xie@utsa.edu; Tel.: +1-210-458-5445; Fax: +1-210-458-4469

Abstract: In arid regions, C3 vegetation is assumed to be more sensitive to precipitation and CO_2 fertilization than C4 vegetation. In this study, normalized difference vegetation index (NDVI) is used to examine vegetation growth in the arid Lower Heihe River Basin, northwestern China, for the past three decades. The results indicate that maximum NDVI (MNDVI) of the area increases over the years and is significantly correlated with precipitation (R = 0.47 and p < 0.01), not temperature (R = −0.04). The upper limit of C3 vegetation cover of the area shows a yearly rising trend of 0.6% or an overall increase of 9% over the period of 25 years, primarily due to the CO_2 fertilization effect (CO_2 rising 14%) over the same period. C3 dominant areas can be potentially distinguished by both MNDVI asynchronous seasonality and a significant relation between MNDVI and cumulative precipitation. This study provides a potential tool of identifying C3 vegetation from C4 vegetation and confirms the CO_2 fertilization effect in this arid region.

Keywords: lower Heihe River Basin; NDVI; climate factors; CO_2 fertilization effect

1. Introduction

As an important indicator in global climate change, vegetation plays a central role in bridging land surface and atmosphere [1]. Global vegetation changes could be the results of a chain-reaction of climatic changes [2]. Typically, climatic factors, CO_2 fertilization, and land-use change have been considered as three primary elements that influence the vegetation coverage in this planet [1,3,4]. Among these factors, temperature and precipitation are the two most important [5,6]. Investigating vegetation response to precipitation and temperature anomalies, particularly during droughts, is of great importance in arid regions, because ecosystem and hydrologic processes in those areas are mostly dependent on vegetation conditions [7,8]. On the other hand, the significant increase of atmospheric CO_2 concentration (from below 300 ppm to almost 400 ppm) in the past 200 years, primarily caused by human activities [9], has resulted in an observable impact on terrestrial vegetation variations [10]. In past decades, rising CO_2 concentrations played a dominant influence on the structure (*i.e.*, floristic composition, canopy cover, height, *etc.*) of vegetation in cold, arid, and high altitude areas [11]. Remote sensing has been an essential tool for mapping land use/cover and for inferring phenological characteristics of vegetation [1]. The normalized difference vegetation index (NDVI) derived from remote sensing data is sensitive to vegetation's chlorophyll content [12], nutrient levels [13], and water content as well as the underlying soil characteristics [14,15]. Therefore, NDVI serves as an effective and simple indicator to evaluate vegetative characteristics on earth's surface. This makes monitoring of photosynthetic vegetative activity in large areas a reality. The correlation of an appropriate indicator for monitoring vegetation cover variations with climate factors (e.g., temperature and precipitation) and CO_2 concentration is key to building better global vegetation

models [3,4,16,17]. Particularly, time-integrated NDVI is commonly used for growth status, spatial density distribution [18–20], and phenology of plants [21,22]. Many studies between NDVI and climatic factors have been conducted in past decades. For example, Ichii *et al.* (2002) identified a significant correlation between NDVI, temperature and precipitation in the northern and southern semiarid regions [23]. Maselli *et al.* (2009) demonstrated that both NDVI annual averages and seasonal variations are strictly dependent on rainfall patterns, particularly in arid zones [24]. Song and Ma (2011) identified that rainfall is the most important climatic factor that closely correlates with NDVI, particularly in arid environments [25].

However, the relationship between CO_2 concentration and vegetation cover is too complex to decipher, since it is not easy to isolate the direct biochemical role of CO_2 concentration as a single factor from other variations such as water, temperature, nutrients, and land use [6,26–28]. Photosynthesis is the process by which plants use sunlight to bond CO_2 and H_2O together to make O_2 and sugar. In arid environments, water use is a limiting factor in determining the photosynthesis efficiency. Especially, at low precipitation levels, the upper limit of vegetation coverage is linearly increased with precipitation levels [29]. In addition, this upper limit is independent of vegetation and climate type [30,31]. Donohue *et al.* (2013) demonstrated that CO_2 concentration plays a key role in setting the upper limit of vegetation cover in arid environments [17]. Despite of the year-to-year variation in precipitation, the upper limit edge of vegetation cover (E_v) increases with the CO_2 concentration due to the rise of water use efficiency of photosynthesis (W_p), which is also referred as the CO_2 fertilization effect [17]. However, whether or not this type of CO_2 effect is transferable to other environments of cold and/or arid is still questionable.

C3 carbon fixation is one of the three pathways for carbon fixation in photosynthesis, along with C4 and Crassulacean acid metabolism (CAM) [32]. Most plants use C3 photosynthesis pathway where the CO_2 is first incorporated into a three-carbon compound. However, this type of photosynthesis is not well-suited to all environments. In arid environments, for example, some plant species use an adaptation, which is C4 photosynthesis that CO_2 is first incorporated into a four-carbon compound. Vegetation following the C3 and C4 photosynthetic pathways can differ greatly in their exchanges of carbon dioxide, water and energy with the atmosphere [33]. It has been suggested that changes in the atmospheric CO_2 level would more likely influence the photosynthetic activities of C3 than of C4 [34]. Increasing CO_2 enhances the response of C3 plants but not C4 plants, because the ambient CO_2 concentration is enough to satisfy the needs of the unique photosynthetic pathway in C4 plants [35–37].

In order to accurately determine the CO_2 fertilization effect, C3 plant areas should be first mapped. Since C3 species are more active than C4 species in the spring and autumn seasons, the green-up date of C3 species is earlier or later than C4 species [33]. Numeric methods have been used to summarize the temporal profiles of vegetation indices including the identification of key dates (e.g., date of onset of greenness or date of maximum greenness) and trends [38,39]. Two most common methods are normally used to distinguish C3 and C4 based on their asynchronous seasonality [39]. The first one is based on the normalized cumulative NDVI (NCNDVI) [40]. According to a comparison study of remote sensing and *in situ* data in south Dakota, USA, 27.5% is a threshold NCNDVI value to distinguish high C3 cover area (coverage is larger than 50%) from C4 cover area [33]. The second one is based on the appearing date of maximum NDVI (MNDVI) with an assumption that C4 plants green mostly in warmer seasons and C3 plants in colder seasons [41].

In this study, the Lower Heihe River Basin (LHRB), a typical arid region in Northwestern China, is used as a test bed to examine whether and how the vegetation cover has changed under the rising CO_2 concentration. The plants in LHRB include C3 plants (*Hedy sarum scoparium*, *Tamarix chinensis Lour*, *Poplar*, *Soybean*, and *Potato*) and C4 plants (*Haloxylon ammodendron*, *Calligonum mongolicum Turcz*, and *Maize*) [42]. It has been implied that a precipitation difference has a great effect on C3/C4 ratios, because C3 plants are more sensitive to precipitation than C4 plants [43]. Therefore, in this study, we propose a method using the correlation coefficient between NDVI and precipitation as a potential indicator to separate C3 from C4 plants. The results are compared with those derived from

the two common methods. The CO_2 fertilization effect is therefore examined based on the edge change of maximum vegetation cover in C3 dominate areas.

2. Study Area

The Heihe River Basin (HRB) is the second largest inland watershed in China. The lower reach of the basin (LHRB) has been intensified due to the water scarcity and has posed a threat to the sustainability of agricultural production and provision of essential ecosystem services such as primary production and soil conservation [44,45]. Since precipitation in LHRB (~37 mm annually) is far less than the water needed for growth of crop and other vegetation in the region, water from the Upper Heihe River (primarily from snow and glacier melts) plays a key role in sustaining the agricultural ecosystem as well as other ecosystems along the river path [46]. However, the river's supply of water to the lower reach has declined sharply due to climate change and unreasonable water utilization in the middle reach of the river basin during past decades and has led to serious vegetation deterioration, shrinkage of natural oases, intensified desertification and frequent sandstorms [47]. This has threatened the provision of ecosystem services essential to human well-being of local people [48]. In the 1980s, the predominant natural vegetation in LHRB were *Populus euphratica* (C3), *Tamarix ramosissima* (intermediate C3/C4), *Haloxylon ammodendron* (C4), *Sophora alopecuroides* (C3), and sparse *Nitraria tangutorum Bobr* (C3) [47]. In recent decades, over-extraction of the groundwater has caused a decline in the water table of the region, resulted in the withering of *Populus euphratica* in large areas [44]. Due to the desertification, *Reaumuria soongorica* (C3) and *Passerina passerina* (C4) became two dominant species in the desert regions of LHRB [49]. Their height and crown diameter change widely with habitats. Both species are super-xerophytic desert plants [50]. Typically, the NDVI value in LHRB is as low as 0.1, which is very sensitive to weather conditions such as precipitation [51].

The LHRB lies between 97.13°–102.12°E and 39.87°–42.79°N (Figure 1), with a total land area of approximately 7.71×10^4 km^2. It is a typical arid region, with the annual precipitation of ~37 mm and the maximum annual evapotranspiration exceeding 1000 mm [52]. Most part of the LHRB is covered by unused land (e.g., sandy land and Gobi desert) and low-coverage vegetation lands. The unused land and low-coverage vegetation accounts for 83% and 14% of the total land area in 2008, respectively [53].

3. Data and Methodology

3.1. Precipitation Data

We use Asian Precipitation Highly-Resolved Observational Data Integration Toward Evaluation (APHRODITE) data for the study. This is the only long-term (1951 onward) continental-scale daily gridded product (25 km cell size) for Asia including the Himalayas, South and Southeast Asia and mountainous areas in the Middle East. The products are available on a regional basis (http://www.chikyu.ac.jp/precip). Considering the growing season ends at the end of September and precipitation after September has no influence on the vegetation growth of the current year, we only calculate the cumulative precipitation from June to September as the growing season precipitation. The precipitation data from 1981 to 2007 is used in this study. One hundred and seventy eight APHRODITE grid cells covering the LHRB (Figure 1) are used to examine the interrelationships between precipitation (P), air temperature (T_{air}), and NDVI.

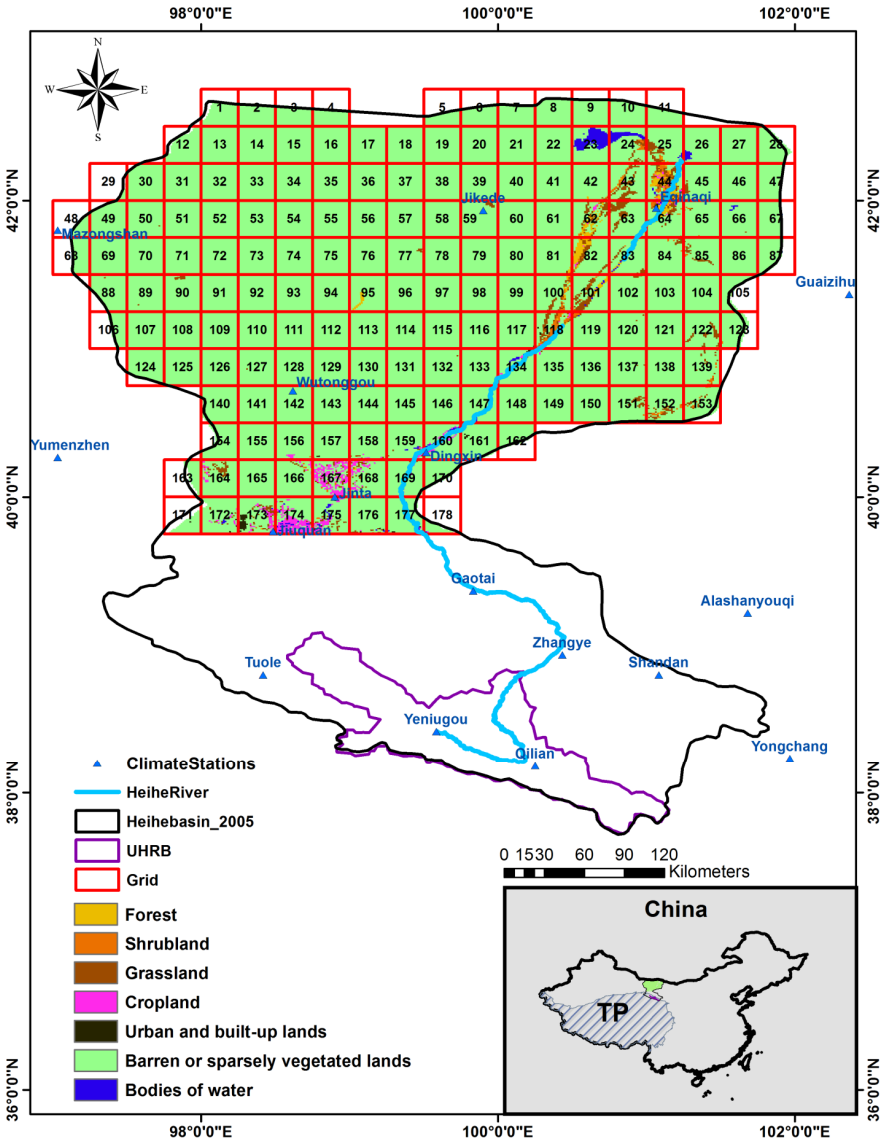

Figure 1. Lower Hehei River Basin (LHRB) (green area), northeast of the Tibetan Plateau (TP), with six weather stations: Eqinaqi (elevation of 940.5 m), Jikede (965.6 m), Wutonggou (1591 m), Dingxin (1177.4 m), Jinta (1270.2 m), and Jiuquan (1477.2 m). The land cover types are from Chinese Western Data Center (http://westdc.westgis.ac.cn/) [53]. The 178 grid cells (25 km × 25 km) of precipitation data with cell identification number (ID) used in the text are shown with red lines.

3.2. NOAA/AVHRR-NDVI Data

Corrected from the Pathfinder NDVI of Advanced Very High Resolution Radiometer (AVHRR) data, the Global Inventory Modeling and Mapping Studies (GIMMS)-NDVI data set with a resolution of 8 km × 8 km has become one of the most commonly used NDVI data sets [54]. Two MNDVI values (maximum value of the first 15 days and maximum value of the remaining days of the month) each month from 1981 to 2012 are used in this study [55,56].

Since the resolution for APHRODITE (25 km × 25 km) is much coarser than that of AVHRR vegetation index (8 km × 8 km), *i.e.*, each APHRODITE grid cell including 16 (4 × 4) AVHRR grid cells (Figure 2), the weighted average NDVI for each APHRODITE cell is calculated based on these 16 AVHRR data. The maximum NDVI of each APHRODITE grid cell during the growing season (April to September) of each year is defined as the maximum NDVI (MNDVI) of the cell for the year.

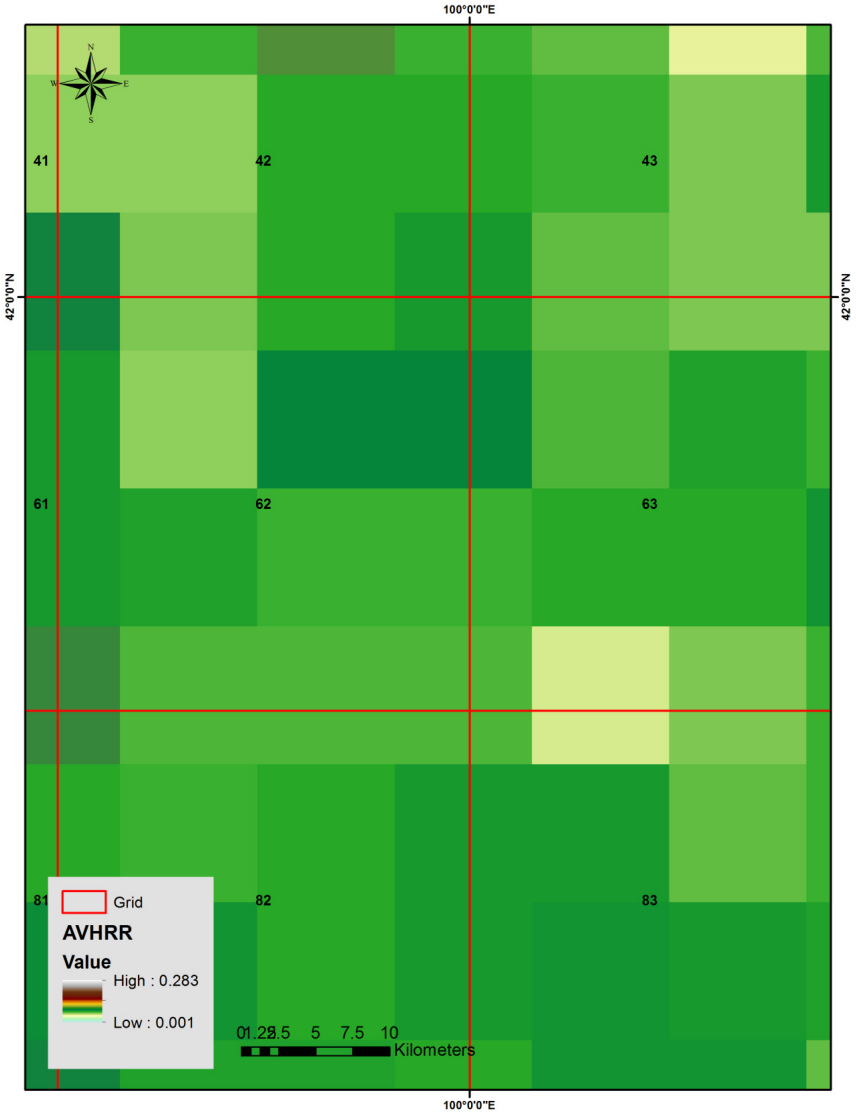

Figure 2. The overlap between APHRODITE (large red cells) and AVHRR NDVI data (small cells), resulting in 16 small cells in each large cell.

3.3. Air Temperature Data

Air temperature (T_{air}) of the LHRB is obtained from six weather stations: Eqinaqi (at elevation of 940.5 m), Jikede (965.6 m), Wutonggou (1591 m), Dingxin (1177.4 m), Jinta (1270.2 m), and Jiuquan (1477.2 m), downloaded from Chinese Western Data Center (http://westdc.westgis.ac.cn/). The elevation range of those stations is between 940.5 m and 1591 m, with mean of 1118.7 m.

3.4. Correlation between Climate Factors and NDVI

The MNDVI values are correlated with the climate factors (mean air temperature in the same month of the MNDVI and cumulative precipitation of two months, *i.e.*, the month of the MNDVI and the month before) at the 178 grid cells, by using Pearson's correlation method for the period of 1981 to 2012. For correlation between air temperature and MNDVI, only the grid cells corresponding with the six weather stations are included for analysis, since there are no temperature data in other cells.

3.5. Discrimination of C3 and C4 Vegetation based on Different Methods

3.5.1. Method 1-Based on Normalized Cumulative NDVI

The seasonal profile of NDVI in each APHRODITE grid over the period is used to derive a cumulative NDVI distribution over each year. First, we define the normalized cumulative NDVI (NCNDVI) as the percentage of cumulative NDVI in the first six months over the total cumulative NDVI in a year as shown in Equation (1) [33].

$$NCNDVI(\%) = \frac{cumulative NDVI\ in\ the\ first\ six\ months}{total\ cumulative NDVI\ in\ a\ year} \times 100 \quad (1)$$

Based on Foody and Dash (2007) in the North America, strong relationships between the grassland composition (C3 and C4) with the NCNDVI were observed (R^2 = 0.59). The NCNDVI increases as the fractional C3 rises. NCNDVI of 27.5% is a value corresponding to 50% of C3 in the grassland. This empirical value indicates that areas with NCNDVI higher than 27.5% are C3 dominant; otherwise, C4 dominant.

3.5.2. Method 2-Based on Date of Maximum NDVI

Table 1 is a look-up table showing the half month numbers, *i.e.*, two NDVI values in each month. The half month of appearance of MNDVI is determined for all the grid cells of each year. Based on the occurring dates/months of MNDVI, it is possible to differentiate the C3 and C4 plants in LHRB. Since C3 plants are cool-season plants and C4 plants are warm-season plants, if the MNDVI in a given area/grid cell occurs in spring season (March to May) or autumn season (September to November), we identify the given area/grid cell as a C3 dominant area; otherwise, if the MNDVI occurs in summer season (June to August), we identify this given area/grid cell as a C4 dominant area [41].

Table 1. Look-up table of half month numbers.

Half Month No.		Half Month No.	
1st half of January	1	1st half of July	13
2nd half of January	2	2nd half of July	14
1st half of February	3	1st half of August	15
2nd half of February	4	2nd half of August	16
1st half of March	5	1st half of September	17
2nd half of March	6	2nd half of September	18
1st half of April	7	1st half of October	19
2nd half of April	8	2nd half of October	20
1st half of May	9	1st half of November	21
2nd half of May	10	2nd half of November	22
1st half of June	11	1st half of December	23
2nd half of June	12	2nd half of December	24

3.5.3. Method 3-Based on Correlation Between MNDVI and Precipitation

The third method, proposed in this study, is based on different sensitivity of C3 and C4 vegetation toward the cumulative precipitation in the month of MNDVI and the month before. It is based on correlation coefficients between MNDVI and accumulative precipitation that is performed in each grid cell from 1981 to 2007 for all years. Based on the assumption that C3 plants are more sensitive to precipitation than C4 plants, for a given grid cell, the higher the correlation coefficients between MNDVI and precipitation, the more likely C3 plants are dominating the given area. That is to say that, if the MNDVI in a given area/grid cell is significantly (p value < 0.01) correlated with the cumulative precipitation of the two months, the given area is then defined as a C3 dominant area; otherwise, the area is defined as a C4 dominant area.

3.6. Quantification of the CO_2 Fertilization Effect

Water use efficiency could be considered as the increase of leaf weight or area with a unit increase of precipitation. Thus, by plotting MNDVI of C3 vegetation against the corresponding precipitation, the slope of the regression line would be approximately considered as the water use efficiency. CO_2 effect is the increase of water use efficiency of photosynthesis (W_p) as the rising of CO_2 concentration, which is based on the Equation (2) developed by Wong *et al.* (1979) [57],

$$\frac{dW_p}{W_p} \approx \frac{dC_a}{C_a} - \frac{1}{2}\frac{dv}{v} \quad (2)$$

where C_a is the atmospheric CO_2 concentration, v is the leaf-to-air water vapor pressure difference. The CO_2 fertilization effect is the increase of W_p as the rise of CO_2 concentration over time.

The CO_2 fertilization effect is calculated only based on C3 plants. The upper limit edge of vegetation cover (E_v edge) is defined as the slope of a linear regression line of MNDVI of C3 plants against cumulative precipitation in the month of the MNDVI and the month before. In order to minimize the impact of year-to-year "transient" effects (e.g., soil water storage change and the response lag of changes in precipitation), we perform the analyses using sequential three-year periods (yielding nine three-year averages between 1981 and 2007). This gives nine separate estimates of E_v. Finally, we test whether the slope of the E_v regression has changed over time.

4. Results

4.1. Characteristics of Temporal Variations of NDVI

As shown in Figure 3a, for an average of annual cycle of NDVI during 1981 to 2012, there is only one broad peak from April to September and the peak appears at the beginning of July and quickly drops down to the lowest value at the end of October. This broad period of April to September corresponds to the growing season for most C3 and C4 vegetation.

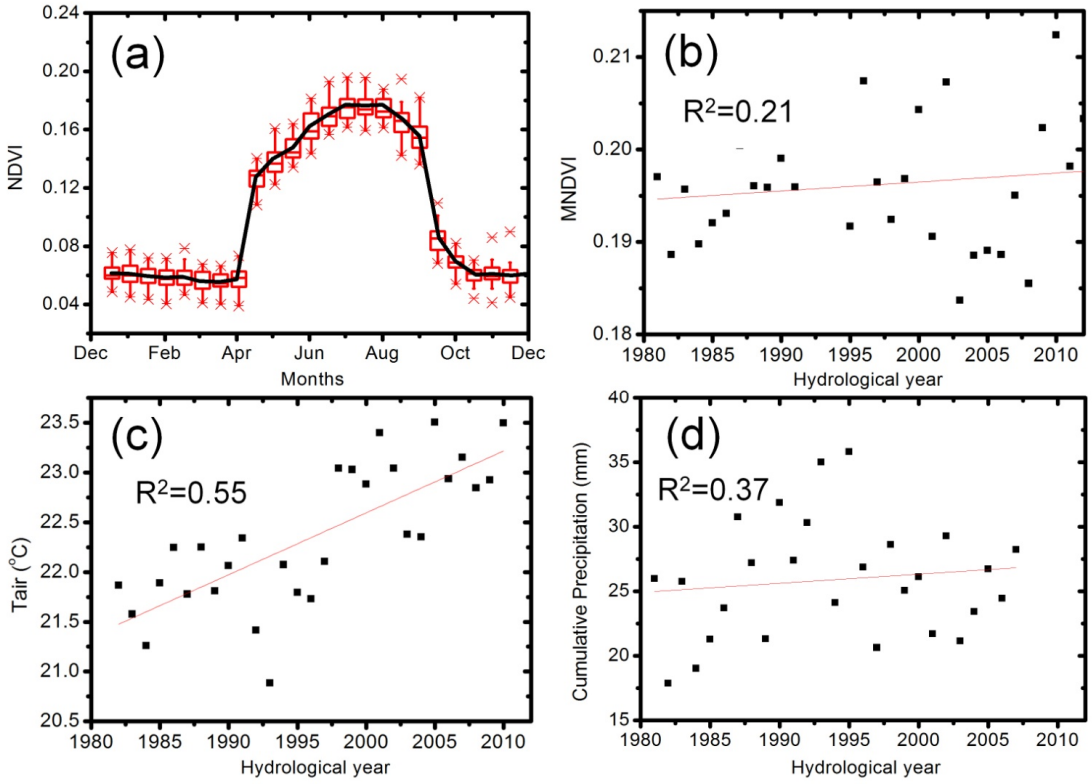

Figure 3. (**a**) Box chart of the monthly mean NDVI of the 22 years from 1981 to 2012 in LHRB and (**b**) the maximum NDVI (MNDVI); (**c**) average air temperature; and (**d**) cumulative precipitation between June and September from 1981 to 2012 in LHRB.

The MNDVI in a growing season shows a slight increase from 1981 to 2012 (Figure 3b). In the same period, the mean air temperature in the growing season shows a strong increase (0.06 °C/year, R^2 = 0.55, p value < 0.01) (Figure 3c), while the cumulative precipitation (June to September) shows strong fluctuations in the range of 16 mm to 37 mm with a slight increase during the period (Figure 3d). Precipitation is positively correlated with MNDVI (R = 0.47, p value < 0.01), while there is no significant correlation between air temperature and MNDVI (R = −0.04). This indicates that in an LHRB area, precipitation is a significant controlling factor of vegetation growth (although only ~22%), but temperature itself is not a direct factor.

4.2. Discrimination of C3 and C4 Vegetation Based on Three Methods

As shown in Figure 4a (Method 1), the NCNDVI values for all the grid cells range from 14.2% to 37.1%, with most of them higher than 30% (*i.e.*, the majority of the grid cells with grid cell identification numbers (IDs) from 1 to 150, the northern area of the LHRB). Based on the 27.5% criteria (*i.e.*, NCNDVI > 27.5% as C3 dominant vegetation), the C3 or C4 dominant grid cells/areas are mapped in Figure 5a). As shown in Figure 4b (Method 2), majority of the grid cells with IDs smaller than 100 (the northern area of the LHRB) have MNDVI values either in (I) the 9th to 10th half months (*i.e.*, the month of May) or (II) the 17th and18th half months (*i.e.*, the month of September), corresponding to MNDVI of C3 vegetation. The rest of them correspond to the MNDVI of C4 vegetation, as mapped in Figure 5b. As shown in Figure 4c (Method 3), the correlation coefficients range from −0.3 to 0.8. Therefore, the areas with significantly high correlation (R > 0.47, p value < 0.01) are selected as the potential C3 species areas (Figure 5c).

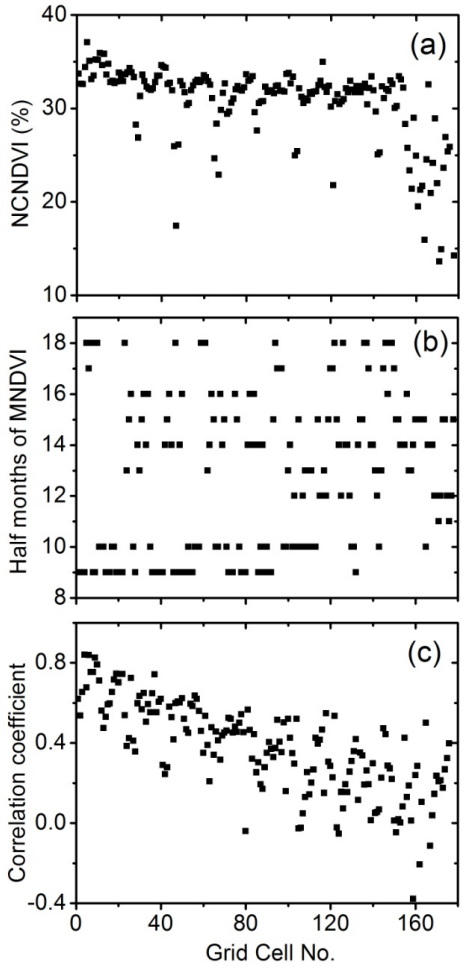

Figure 4. (**a**) The normalized cumulative NDVI (NCNDVI), (**b**) the maximum NDVI (MNDVI); and (**c**) the correlation coefficient between MNDVI and precipitation in the 178 grid cells (note: grid cell number is the grid cell ID as shown in Figure 1).

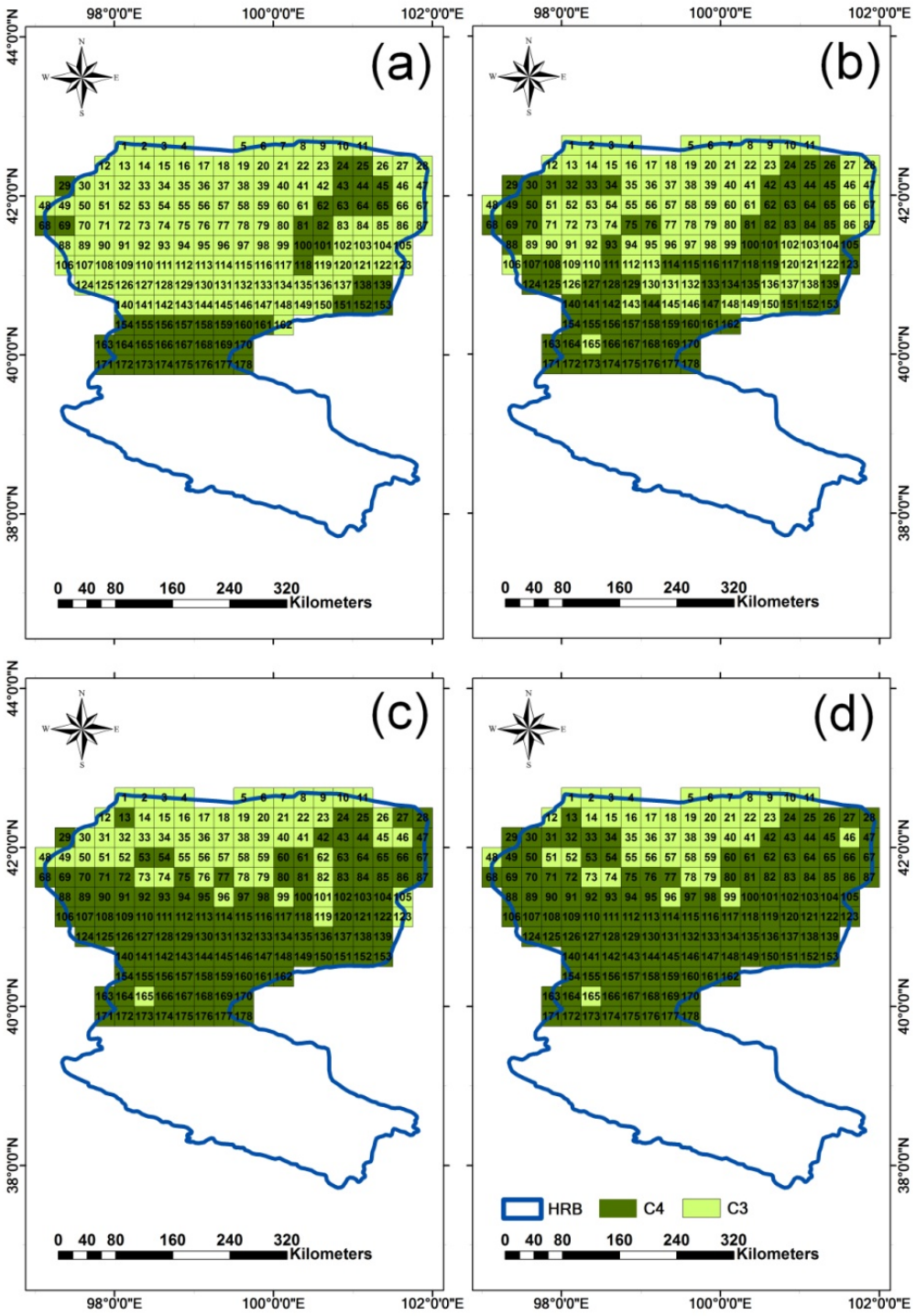

Figure 5. Potential C3 dominant areas determined by (**a**) normalized cumulative NDVI (method 1), (**b**) maximum NDVI (method 2); and (**c**) significant correlation with precipitation (method 3); and (**d**) overlapping C3 dominant areas of (b) and (c).

The results based on the three methods have a common feature: C3 plants are more prevalent in the northern part of LHRB than in the southern part of LHRB. Usually, C3 plants favor the cold environment (colder in the higher latitudes); therefore, the overall trend of C3 and C4 distributions of these three methods seem reasonable. Noting that the coverage of C3 dominant areas based on method 1 is much larger than that of the other two methods. The overlapping C3 dominant areas based on the methods 2 and 3 are shown in Figure 5d, which is used to quantify CO_2 fertilization effects.

4.3. Quantification of CO_2 Fertilization Effect

Although the fluctuation of the slope of upper limit edge of vegetation cover (E_v) is observed, the overall trend shows a yearly rising of 0.6% over 25 years (Figure 6a). The Figure 6b is a plot of MNDVI against corresponding cumulative precipitation for the year 1981 (black) and year 2007 (red). The relative increase is about 9% (Figure 6b), which is close to the 14% increase of global CO_2 concentration (from satellite estimations) over the same period [58].

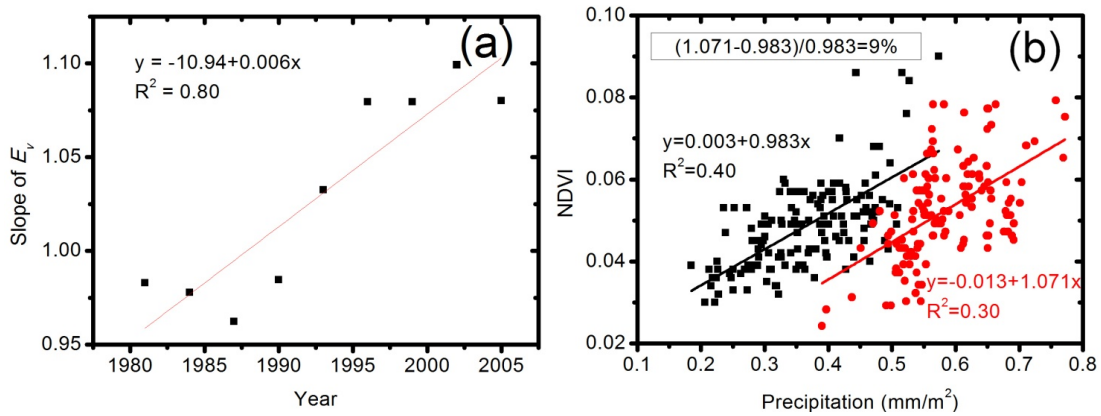

Figure 6. (**a**) Trend of Slope of E_v from 1981 to 2007 and (**b**) Slope of E_v in 1981 (black) and 2007 (red), with a relative increasing rate of 9%.

5. Discussion

In this paper, we examine the relationship between NDVI and precipitation/temperature in LHRB, as well as their spatial distributions. The results are as follows: (1) The NDVI value reaches the maximum from April to September; (2) C3 species could be distinguished from C4 species by both NDVI asynchronous seasonality and correlation coefficients between MNDVI and precipitation; (3) C3 species show statistically significant correlation between MNDVI and precipitation from 1981 to 2007; and (4) the change of slope of E_v (9%) is attributed to the CO_2 fertilization effect, *i.e.*, the 14% increase in CO_2 concentration over the same period of time.

Comparing the results determined by these three methods used in this study (Figure 5), it is found that the C3 vegetation mapped by method 1 seems to be too much. Realizing that method 1 is based on a semi-empirical threshold value (NCNDVI larger than 27.5%) estimated in USA, the direct application of this value to the study area could be questionable. Although time-integrated NDVI has been used as one of the most useful parameters to represent the greenness of the growth cycle and has been effectively mapped the C3/C4 composition of grasslands, the generality of the methodology has never been proven outside the central North America [59]. Considering that the seasonal response of C3 and C4 species to climate drivers (such as precipitation and temperature), the North American prairie would be different from that in northwestern China. The climate condition in LHRB is also quite different from the North America, the approach (*i.e.*, the threshold value) to map C3 and C4 grasses developed in North America could be the least accurate in LHRB. In particular, most of the "C3 dominant areas" determined by the method 1 (*i.e.*, mapped C3 grid cells in Figure 5a) show poor correlation with precipitation (*i.e.*, mapped C4 grid cells in Figure 5c).

Both methods 2 and 3 are based on the site specific characteristics of C3 and C4 plants. The results based on method 3 show that there are only a small portion of areas in the north part of LHRB would be C3 plants. Most of these areas also match the C3 plants areas determined by the second method, which is based on the asynchronous seasonality (maximum greenness date). Thus, the combination of these two methods would give the most reliable discrimination of C3 and C4 dominant areas. Thus, the overlapping C3 dominant areas between the method 2 and method 3 are defined as the potential C3 areas (Figure 5d) for studying the CO_2 fertilization effect. However, further ground investigation is needed to justify the validation of these results.

As we mentioned earlier, precipitation only explains ~22% of NDVI increase, the increasing CO_2 may explain the remaining over 70% of NDVI increase. Burges *et al.* (1991) discovered that the size and dry weight of most C3 plants and plant components would increase under rising CO_2 concentration because relatively more photo-assimilation is partitioned into structural components (stems and petioles) during vegetative development in order to support the light-harvesting apparatus (leaves) [60]. These results can be explained reasonably by three assumptions: (a) the C3 plant areas chosen by the combination of methods 2 and 3 are under sustained CO_2 fertilization effect; (b) the change rate of CO_2 concentration is constant in the LHRB area from 1982 to 2012; and (c) the LHRB area is so limited in water availability that the change in CO_2 concentration might be predominantly expressed through transpiration, with little change in assimilation. This result also provides strong support for our hypothesis that the E_v edge of C3 vegetation is, in large part at least, determined by CO_2. By implication, analyzing the changes in the E_v edge provides a means for assessing the CO_2 fertilization effect as it has historically occurred across the globe's warm and arid landscapes.

If we simply consider that the maximum NDVI as a function of precipitation and CO_2 concentration, the most effective analysis technique is to remove the effects of variability in precipitation, taking a derivative of NDVI, which is equivalent to E_v. Across the study area and time period, the precipitation-induced greening cannot fully explain the increase of the slope in the E_v. To evaluate the CO_2 fertilization effect, we only consider the C3 dominated areas and make sure of linearity between maximum NDVI and precipitation level. Although our result indicates the CO_2 fertilization effect on the increased greenness in LHRB, other factors in plant growth such as availability of nutrients (nitrogen and phosphorous) could also be important [61,62]. Future field study is required to warrant the availability of nitrogen and phosphorous in the LHRB area.

6. Conclusions

As an important supplement for the previous study of CO_2 fertilization effect in warm and arid areas, we have demonstrated the increase of water use efficiency of photosynthesis with rising CO_2 concentration in the Lower Heihe River Basin (LHRB), a typical cold and arid area in China. The extremely arid climate condition of LHRB makes it an ideal place for studying CO_2 fertilization effect. Our result indicates that the increasing CO_2 level may explain over 70% of NDVI increase. C3 dominant areas can be potentially distinguished by both MNDVI asynchronous seasonality and significant relation between MNDVI and cumulative precipitation. This finding could facilitate better understanding of the impact of climate change on vegetation variation in arid or semi-arid areas. However, validation of the methods in other interesting areas (such as the Chihuahua Desert in Mexico and USA) is eagerly needed.

Acknowledgments: The work was partially supported by the Chinese Academy of Sciences Action Plan for West Development Program Project "Remote Sensing Data Products in the Heihe River Basin: Algorithm Development, Data Products Generation and Application Experiments" (KZCX2-XB3-15); Y. Bi thanks the assistantship support from the Environment Science and Engineering PhD program at the University of Texas at San Antonio and a NASA grant *(NX11AE42G)*. We would like to acknowledge the U.S. NOAA for the provision of AVHRR-NDVI data, the China Meteorological Data Sharing Service System for the station data, and APHRODITE's Water Resources in Japan for the precipitation data. We would like to thank the constructional comments from three anonymous reviewers to improve the paper.

Author Contributions: Yunbo Bi collected and processed the data, analyzed and explained the results. Hongjie Xie designed the project idea and methodology and guided the data/result interpretation and conclusion development. Yunbo Bi wrote the paper with help and guidance from Hongjie Xie. All coauthors contributed to the paper review and revisions.

Conflicts of Interest: The authors declare no conflict of interest.

References

1. Han, H.; Ma, M.; Yan, P.; Song, Y. Periodicity analysis of NDVI time series and its relationship with climatic factors in the Heihe River Basin in China. *Proc. SPIE* **2011**, doi:10.1117/12.897938.
2. Deil, U. A review on habitats, plant traits and vegetation of ephemeral wetlands—A global perspective. *Phytocoenologia* **2005**, *35*, 533–705.
3. Bennett, K.D.; Willis, K.J. Effect of global atmospheric carbon dioxide on glacial-interglacial vegetation change. *Glob. Ecol. Biogeogr.* **2000**, *9*, 355–361.
4. Kidane, Y.; Stahlmann, R.; Beierkuhnlein, C. Vegetation dynamics, and land use and land cover change in the Bale Mountains, Ethiopia. *Environ. Monit. Assess.* **2012**, *184*, 7473–7489.
5. Fang, J.Y.; Piao, S.L.; He, J.S.; Ma, W.H. Increasing terrestrial vegetation activity in China, 1982–1999. *Sci. China Ser. C Life Sci.* **2004**, *47*, 229–240.
6. Nemani, R.R.; Keeling, C.D.; Hashimoto, H.; Jolly, W.M.; Piper, S.C.; Tucker, C.J.; Myneni, R.B.; Running, S.W. Climate-driven increases in global terrestrial net primary production from 1982 to 1999. *Science* **2003**, *300*, 1560–1563.
7. Porporato, A.; Daly, E.; Rodriguez-Iturbe, I. Soil water balance and ecosystem response to climate change. *Am. Nat.* **2004**, *164*, 625–632.
8. Canon, J.; Dominguez, F.; Valdes, J.B. Vegetation responses to precipitation and temperature: A spatiotemporal analysis of ecoregions in the Colorado River Basin. *Int. J. Remote Sens.* **2011**, *32*, 5665–5687.
9. IPCC. *Climate Change 2013: The Physical Science Basis. Working Group I Contribution to the Fifth Assessment Report of the Intergovernmental Panel on Climate Change*; Cambridge University Press: Cambridge, UK; New York, NY, USA, 2013; p. 1535.
10. Port, U.; Brovkin, V.; Claussen, M. The influence of vegetation dynamics on anthropogenic climate change. *Earth Syst. Dyn.* **2012**, *3*, 233–243.
11. Qiu, L.; Liu, X. Sensitivity analysis of modelled responses of vegetation dynamics on the Tibetan Plateau to doubled CO_2 and associated climate change. *Theor. Appl. Climatol.* **2015**, 1–11, doi:10.1007/s00704-015-1414-1.
12. Daughtry, C.S.T.; Walthall, C.L.; Kim, M.S.; de Colstoun, E.B.; McMurtrey, J.E. Estimating corn leaf chlorophyll concentration from leaf and canopy reflectance. *Remote Sens. Environ.* **2000**, *74*, 229–239.
13. Song, X.Y.; Wang, J.H.; Yang, G.J.; Feng, H.K. Winter wheat cropland grain protein content evaluation through remote sensing. *Intell. Autom. Soft Comput.* **2014**, *20*, 599–609.
14. Wang, X.W.; Xie, H.J.; Guan, H.D.; Zhou, X.B. Different responses of MODIS-derived NDVI to root-zone soil moisture in semi-arid and humid regions. *J. Hydrol.* **2007**, *340*, 12–24.
15. Schnur, M.T.; Xie, H.J.; Wang, X.W. Estimating root zone soil moisture at distant sites using MODIS NDVI and EVI in a semi-arid region of southwestern USA. *Ecol. Inform.* **2010**, *5*, 400–409.
16. Murray, S.J.; Foster, P.N.; Prentice, I.C. Future global water resources with respect to climate change and water withdrawals as estimated by a dynamic global vegetation model. *J. Hydrol.* **2012**, *448*, 14–29.
17. Donohue, R.J.; Roderick, M.L.; McVicar, T.R.; Farquhar, G.D. Impact of CO_2 fertilization on maximum foliage cover across the globe's warm, arid environments. *Geophys. Res. Lett.* **2013**, *40*, 3031–3035.
18. Gessner, U.; Naeimi, V.; Klein, I.; Kuenzer, C.; Klein, D.; Dech, S. The relationship between precipitation anomalies and satellite-derived vegetation activity in Central Asia. *Glob. Planet. Chang.* **2013**, *110*, 74–87.
19. Barichivich, J.; Briffa, K.R.; Myneni, R.B.; Osborn, T.J.; Melvin, T.M.; Ciais, P.; Piao, S.L.; Tucker, C. Large-scale variations in the vegetation growing season and annual cycle of atmospheric CO_2 at high northern latitudes from 1950 to 2011. *Glob. Chang. Biol.* **2013**, *19*, 3167–3183.
20. Hu, M.Q.; Mao, F.; Sun, H.; Hou, Y.Y. Study of normalized difference vegetation index variation and its correlation with climate factors in the three-river-source region. *Int. J. Appl. Earth Observ. Geoinf.* **2011**, *13*, 24–33.
21. Meier, G.A.; Brown, J.F. Remote sensing of land surface phenology. *US Geol. Surv.* **2014**, doi.org/10.3133/fs20143052.
22. Rigge, M.; Smart, A.; Wylie, B.; Gilmanov, T.; Johnson, P. Linking phenology and biomass productivity in South Dakota mixed-grass prairie. *Rangel. Ecol. Manag.* **2013**, *66*, 579–587.
23. Ichii, K.; Kawabata, A.; Yamaguchi, Y. Global correlation analysis for NDVI and climatic variables and NDVI trends: 1982–1990. *Int. J. Remote Sens.* **2002**, *23*, 3873–3878.
24. Maselli, F.; di Gregorio, A.; Capecchi, V.; Breda, F. Enrichment of land-cover polygons with eco-climatic information derived from MODIS NDVI imagery. *J. Biogeogr.* **2009**, *36*, 639–650.

25. Song, Y.; Ma, M.G. A statistical analysis of the relationship between climatic factors and the Normalized Difference Vegetation Index in China. *Int. J. Remote Sens.* **2011**, *32*, 3947–3965.
26. Beck, H.E.; McVicar, T.R.; van Dijk, A.I.J.M.; Schellekens, J.; de Jeu, R.A.M.; Bruijnzeel, L.A. Global evaluation of four AVHRR-NDVI data sets: Intercomparison and assessment against Landsat imagery. *Remote Sens. Environ.* **2011**, *115*, 2547–2563.
27. Fensholt, R.; Langanke, T.; Rasmussen, K.; Reenberg, A.; Prince, S.D.; Tucker, C.; Scholes, R.J.; Le, Q.B.; Bondeau, A.; Eastman, R.; *et al*. Greenness in semi-arid areas across the globe 1981–2007—An Earth Observing Satellite based analysis of trends and drivers. *Remote Sens. Environ.* **2012**, *121*, 144–158.
28. Houghton, R.A. Revised estimates of the annual net flux of carbon to the atmosphere from changes in land use and land management 1850–2000. *Tellus Ser. B Chem. Phys. Meteorol.* **2003**, *55*, 378–390.
29. Ghannoum, O. C-4 photosynthesis and water stress. *Ann. Bot.* **2009**, *103*, 635–644.
30. Huxman, T.E.; Smith, M.D.; Fay, P.A.; Knapp, A.K.; Shaw, M.R.; Loik, M.E.; Smith, S.D.; Tissue, D.T.; Zak, J.C.; Weltzin, J.F.; *et al*. Convergence across biomes to a common rain-use efficiency. *Nature* **2004**, *429*, 651–654.
31. Campos, G.E.P.; Moran, M.S.; Huete, A.; Zhang, Y.; Bresloff, C.; Huxman, T.E.; Eamus, D.; Bosch, D.D.; Buda, A.R.; Gunter, S.A.; *et al*. Ecosystem resilience despite large-scale altered hydroclimatic conditions. *Nature* **2013**, *494*, 349–352.
32. Hogan, C.M. Respiration. In *Encyclopedia of Earth*; McGinley, M., Cleveland, C.J., Eds.; National Council for Science and the Environment: Washington, DC, USA, 2011.
33. Foody, G.M.; Dash, J. Discriminating and mapping the C3 and C4 composition of grasslands in the northern Great Plains, USA. *Ecol. Inform.* **2007**, *2*, 89–93.
34. Ehleringer, J. The influence of atmospheric CO_2, temperature, and water on the abundance of C3/C4 taxa. In *A History of Atmospheric CO_2 and Its Effects on Plants, Animals, and Ecosystems*; Baldwin, I.T., Caldwell, M.M., Heldmaier, G., Jackson, R., Lange, O.L., Mooney, H.A., Schulze, E.D., Sommer, U., Ehleringer, J., Dearing, M., *et al*., Eds.; Springer: New York, NY, USA, 2005; pp. 214–231.
35. Kakani, V.G.; Reddy, K.R. Temperature response of C4 species big bluestem (*Andropogon gerardii*) is modified by growing carbon dioxide concentration. *Environ. Exp. Bot.* **2007**, *61*, 281–290.
36. Mishra, R.S.; Abdin, M.Z.; Uprety, D.C. Interactive effects of elevated CO_2 and moisture stress on the photosynthesis, water relation and growth of Brassica species. *J. Agron. Crop Sci.* **1999**, *182*, 223–229.
37. Li, Z.; Zhang, Y.; Yu, D.; Zhang, N.; Lin, J.; Zhang, J.; Tang, J.; Wang, J.; Mu, C. The influence of precipitation regimes and elevated CO_2 on photosynthesis and biomass accumulation and partitioning in seedlings of the rhizomatous perennial grass *Leymus chinensis*. *PLoS ONE* **2014**, *9*, doi:10.1371/journal.pone.0103633.
38. Adjorlolo, C.; Mutanga, O.; Cho, M.A.; Ismail, R. Challenges and opportunities in the use of remote sensing for C-3 and C-4 grass species discrimination and mapping. *Afr. J. Range Forage Sci.* **2012**, *29*, 47–61.
39. Ricotta, C.; Reed, B.C.; Tieszen, L.T. The role of C-3 and C-4 grasses to interannual variability in remotely sensed ecosystem performance over the US Great Plains. *Int. J. Remote Sens.* **2003**, *24*, 4421–4431.
40. Goodin, D.G.; Henebry, G.M. A technique for monitoring ecological disturbance in tallgrass prairie using seasonal NDVI trajectories and a discriminant function mixture model. *Remote Sens. Environ.* **1997**, *61*, 270–278.
41. Sage, R.F.; Kubien, D.S. The temperature response of C-3 and C-4 photosynthesis. *Plant Cell Environ.* **2007**, *30*, 1086–1106.
42. Ran, Y.H.; Li, X.; Lu, L.; Li, Z.Y. Large-scale land cover mapping with the integration of multi-source information based on the Dempster-Shafer theory. *Int. J. Geogr. Inf. Sci.* **2012**, *26*, 169–191.
43. Zhou, B.; Zheng, H.; Shen, C.; Wei, G.; Li, L. Effect of temperature and precipitation on C3/C4 plants evolutions since late Quaternary in the East Asian Monsoon Area: Evidence from carbon isotopes of alkanes and elemental carbon. *AGU Fall Meet. Abstr.* **2009**, *1*, 1394.
44. Guo, Q.; Feng, Q.; Li, J. Environmental changes after ecological water conveyance in the lower reaches of Heihe River, northwest China. *Environ. Geol.* **2009**, *58*, 1387–1396.
45. Qin, D.; Zhao, Z.; Han, L.; Qian, Y.; Ou, L.; Wu, Z.; Wang, M. Determination of groundwater recharge regime and flowpath in the Lower Heihe River basin in an arid area of Northwest China by using environmental tracers: Implications for vegetation degradation in the Ejina Oasis. *Appl. Geochem.* **2012**, *27*, 1133–1145.
46. Yan, H.; Zhan, J.; Liu, B.; Yuan, Y. Model estimation of water use efficiency for soil conservation in the lower Heihe River Basin, Northwest China during 2000–2008. *Sustainability* **2014**, *6*, 6250–6266.

47. Wang, P.; Zhang, Y.; Yu, J.; Fu, G.; Ao, F. Vegetation dynamics induced by groundwater fluctuations in the lower Heihe River Basin, northwestern China. *J. Plant Ecol.* **2011**, *4*, 77–90.
48. Xi, H.; Feng, Q.; Si, J.; Chang, Z.; Cao, S. Impacts of river recharge on groundwater level and hydrochemistry in the lower reaches of Heihe River Watershed, northwestern China. *Hydrogeol. J.* **2010**, *18*, 791–801.
49. Su, P.; Yan, Q.; Xie, T.; Zhou, Z.; Gao, S. Associated growth of C3 and C4 desert plants helps the C3 species at the cost of the C4 species. *Acta Physiol. Plant.* **2012**, *34*, 2057–2068.
50. Su, P.; Yan, Q. Stable carbon isotope variation in plants and their indicating significances along the inland Heihe River basin of northwestern China. *Acta Ecol. Sin.* **2008**, *28*, 1616–1624.
51. Yin, D.; Li, X.; Huang, Y.; Si, Y.; Bai, R. Identifying vegetation dynamics and sensitivities in response to water resources management in the Heihe River Basin in China. *Adv. Meteorol.* **2015**, *2015*, 12, doi:10.1155/2015/861928.
52. Wen, X.; Wu, Y.; Su, J.; Zhang, Y.; Liu, F. Hydrochemical characteristics and salinity of groundwater in the Ejina Basin, Northwestern China. *Environ. Geol.* **2005**, *48*, 665–675.
53. Wang, J.H.; Gai, C.M.; Zhao, J.; Hu, X.L. *Landuse/Landcover Data of the Heihe River Basin in 2011*; Heihe Plan Science Data Center: Lanzhou, China, 2014; doi:10.3972/heihe.039.2014.db.
54. Tucker, C.J.; Pinzon, J.E.; Brown, M.E.; Slayback, D.A.; Pak, E.W.; Mahoney, R.; Vermote, E.F.; el Saleous, N. An extended AVHRR 8-km NDVI dataset compatible with MODIS and SPOT vegetation NDVI data. *Int. J. Remote Sens.* **2005**, *26*, 4485–4498.
55. Liu, G.; Liu, H.; Yin, Y. Global patterns of NDVI-indicated vegetation extremes and their sensitivity to climate extremes. *Environ. Res. Lett.* **2013**, *8*, doi:10.1088/1748-9326/8/2/025009.
56. Pinzon, J.E.; Tucker, C.J. A Non-Stationary 1981–2012 AVHRR NDVI3g Time Series. *Remote Sens.* **2014**, *6*, 6929–6960.
57. Wong, S.; Cowan, I.; Farquhar, G. Stomatal conductance correlates with photosynthetic capacity. *Nature* **1979**, *282*, doi:10.1038/282424a0.
58. Tans, P.; Keeling, R. *Trends in Atmospheric Carbon Dioxide*; National Oceanic & Atmospheric Administration, Earth system Research Laboratory of Global Monitoring Division: Boulder, CO, USA, 2011.
59. Guan, L.; Liu, L.; Peng, D.; Hu, Y.; Jiao, Q.; Liu, L. Monitoring the distribution of C3 and C4 grasses in a temperate grassland in northern China using moderate resolution imaging spectroradiometer normalized difference vegetation index trajectories. *J. Appl. Remote Sens.* **2012**, *6*, doi:10.1117/1.JRS.6.063535.
60. National Research Council (US); Committee on Climate Uncertainty, and Water Resources Management. *Managing Water Resources in the West Under Conditions of Climate Uncertainty: Proceedings of a Colloquium, November 14-16, 1990, Scottsdale, Arizona*; National Academies Press: Washington, DC, USA, 1991.
61. Boelman, N.T.; Stieglitz, M.; Griffin, K.L.; Shaver, G.R. Inter-annual variability of NDVI in response to long-term warming and fertilization in wet sedge and tussock tundra. *Oecologia* **2005**, *143*, 588–597.
62. Boelman, N.T.; Stieglitz, M.; Rueth, H.M.; Sommerkorn, M.; Griffin, K.L.; Shaver, G.R.; Gamon, J.A. Response of NDVI, biomass, and ecosystem gas exchange to long-term warming and fertilization in wet sedge tundra. *Oecologia* **2003**, *135*, 414–421.